BRAIN TUMOUR DETECTION USING HOG BY SVM

Submitted by
Praveena Pedapati

Rama Vaishnavi Tanneedi

Department of Applied Signal processing
Blekinge Institute of Technology
SE-371 79 Karlskrona Sweden

This thesis is submitted to the Department of Applied Signal Processing at Blekinge Institute of Technology in partial fulfilment of the requirements for the degree of Master of Science in Electrical Engineering with Emphasis on Signal Processing.

Contact Information:
Author(s):
Rama Vaishnavi Tanneedi
E-mail: rata16@student.bth.se,
        vaishu1822@gmail.com
Praveena Pedapati
E-mail: prpe16@student.bth.se,
        Praveena_560@gmail.com

Supervisor:
Irina Gertsovich

University Examiner:
Dr. Sven Johansson

ABSTRACT

Detection of a brain tumour in medical images is always a challenging task. Factors like size, shape, and position of tumour vary from different patient's brain. So, it's important to know the exact shape, size and position of a tumour in the brain making it a challenging task for detection. Some patients exhibit high glioma (HG) type tumor while others show low glioma (LG) type. So, knowing the detailed properties of a tumour to detect them in medical images is mandatory.

So far many algorithms have been implemented on how to detect and extract the tumours in medical images, they used techniques such as hybrid approach with Support Vector Machine (SVM), back propagation and dice coefficient. Among these algorithm which used back propagation as base classifier had a highest accuracy of 90%.

In this work feature extraction of the medical images of patients' tumors in database is extracted using Histogram of Oriented Gradient, later these images are classified into tumor and non tumor images using SVM.

The detection of brain tumours in patient's image is achieved by testing the performance of SVM based on Receiver Operating Characteristics (ROC). ROC include true positive rate, true negative rate, false positive rate and false negative rate. Using ROC we calculated accuracy, sensitivity and specificity values for all the medical images of the database. For image data folder of HG in vector form, SVM gave an accuracy of 97% for 95th slice of T1 modality with high true positive rate of 0.97 remaining highest among other modalities. Whereas SVM gave an accuracy of 87% for 135th slice of T1 modality with high true positive rate of 0.8 and low false positive rate of 0.06 among other image data folder of HG. For image data folder of LG, SVM gave an accuracy of 62% for the 90th slice of FLAIR modality with the high true positive rate of 0.5 and low false positive rate of 0.25 among all others. For synthetic data folder of HG, SVM gave an accuracy of 62% for a 100th slice of FLAIR modality with the high true positive rate of 0.5 and low false positive rate of 0.06 among all others. For synthetic data folder of LG, SVM gave an accuracy of 62% for a 100th slice of FLAIR modality with the high true positive rate of 0.5 and low false positive rate of 0.06 among all others.

KEYWORDS: Accuracy, Gradient, Histogram, Sensitivity, Specificity and True positive rate

ACKNOWLEDGEMENTS

Firstly, we would like to offer our gratitude and acknowledgement to our supervisor Irina Gertsovich for her immense support at every stage of our thesis despite her busy schedule. She always guided us in the right way by providing us with valid suggestions, from selecting the topic to clarifying our doubts. She helped us achieve the results with great ease.

We would also like to thank our professors at Blekinge Tekniska Hogskola for guiding us through one and half years of the master degree to achieve the required knowledge to do this work.

Finally, we would like to express our immense gratitude to our parents for their constant encouragement throughout our study, work and writing this thesis.

CONTENTS

LIST OF FIGURES

LIST OF FLOW CHARTS

LIST OF TABLES

ACRONYMS

BRATS/BraTS	BRAIN TUMOR SEGMENTATION
FLAIR	FLUID ATTENUATED INVERSION RECOVERY
FP	FALSE POSITIVE
FN	FALSE NEGATIVE
HG	HIGH GLIOMA
HOG	HISTOGRAM OF ORIENTED GRADIENT
ID	IMAGE DATA
LG	LOW GLIOMA
MRI	MAGNETIC RESONANCE IMAGE
NN	NEURAL NETWORKS
RF	RADIO FREQUENCY
ROC	RECEIVER OPERATING CHARACTERISTICS
SD	SYNTHETIC DATA
SVM	SUPPORT VECTOR MACHINE
TP	TRUE POSITIVE
TN	TRUE NEGATIVE

CHAPTER 1. INTRODUCTION

Detection of a brain tumour from medical images has been a challenging task. The brain is one of the important organs of the human body as it coordinates each and every action of the human body. The human brain can be affected by many diseases like infections, strokes and tumours. A brain tumour is a cancerous or non-cancerous mass or growth of abnormal cells in the brain. It can be termed as the cells which don't die but grows in size and accumulates as a mass [1].

A brain tumour is classified as a primary and secondary tumour. A tumour that starts in the brain is called Primary Brain a tumour. It can be either malignant (contain cancer cells) or benign (do not contain cancer cells). If a cancerous tumour which starts elsewhere in the body sends cells which end up growing in the brain, such tumour is called secondary or metastatic brain tumour [2]. Image testing of a brain tumour is done using x-rays, strong magnets, or radioactive substances to create pictures of the brain [3]. The brain tumours are generally diagnosed using different types of scans. Magnetic Resonance Imaging, Computer Tomography, Angiogram, Myelogram and Positron Emission Tomography are among the types of scans which are used most often to detect brain diseases. These pictures are so efficient that they can provide with primary information about the presence and location of a tumour [4].

COMPUTED TOMOGRAPHY (CT) SCAN:

A Computer Tomography (CT) scan uses X-rays to give a three-dimensional image of the brain. CT scan takes many images instead of taking only one image as in x-ray. CT scanner rotates around you while you lie on a table. Later all these images are combined into images of slices of the body. CT scan gives information of the tumour size and any damage to the bones inside the skull [4].

CT ANGIOGRAM (CTA):

Angiogram uses a series of X-rays to show the arteries and blood vessels of the brain. For the test, you are injected with a contrast material through an IV line while you are in the CT scanner. The scan helps the doctors plan surgery because it can provide better details of the blood vessels in and around a tumour [4].

MYELOGRAM:

Myelogram makes use of a dye to find out whether a tumour has spread to near parts of the body like a spinal cord. The test is done by injecting the dye into Cerebro Spinal Fluid (CSF) [4].

POSITRON EMISSION TOMOGRAPHY (PET) SCAN:

For the test, a radioactive substance called as FDG is injected into the blood. A little amount of FDG is injected so, it passes out of the body within a day or so. Tumour cells in the body grow quickly, so they absorb larger amounts of the sugar than most other cells. After about an hour, you are moved onto a table in the PET scanner. A special camera creates a picture of areas of radioactivity in the body of the patient.

PET scans are not so detailed but they provide information whether abnormal areas seen on other tests are tumours or not [4].

PET scan and CT scan are performed in combination to check whether a tumour has been cured or come back after the treatment. The PET-CT scan is generally performed first as a part of treatment.

MAGNETIC RESONANCE IMAGING (MRI) SCAN:

MRI is the basic diagnosed scan among the types of scans.MRI uses radio waves and strong magnetic fields instead of X-rays. The energy from the radio waves is absorbed and then released in a pattern formed by the type of body tissue and by certain diseases. A computer translates the pattern into a very detailed image of parts of the body. The scan uses a dye which is a contrast material called gadolinium that is injected into the patient's veins before the scan for better details [4].

WHY MRI SCANNED IMAGES ARE PREFERRED COMPARED TO OTHER IMAGING TECHNIQUES?

- ❖ MRI is non-invasive.
- ❖ MRI is cost effective.
- ❖ Good contrasts of the tumours that are present in the brain are provided.
- ❖ Acquisition time (Total body scan) of MRI is less compared to PET and X-Ray.
- ❖ MRI provides better details of bone structure and organs behind them like lungs behind ribs and brain beneath the skull.

1.1 AIM AND OBJECTIVE

The aim of the thesis is to detect the presence of a tumour in the brain images. The main objective is to classify the tumours and non-tumours correctly using SVM (Support Vector Machine). SVM classifies tumour and non-tumour with the feature extraction algorithm HOG (Histogram of Oriented Gradients).

Our objectives include:

a) Select necessary MRI of a brain tumour from a database that needs to be enhanced.

b) Extract the features of the brain tumours using feature extraction algorithm HOG.

c) Extracted feature vectors as the input to SVM for feature vector classification.

d) Evaluate the performance of SVM using the receiver output characteristics (ROC).

1.2 RESEARCH QUESTION

RQ1. How can we classify the brain tumours?

RQ2. Can we detect a tumour in the brain using the feature extraction method HOG?

RQ3. Can SVM classify the tumours and non-tumours correctly?

RQ4. Can we achieve a 100 percent accuracy in classifying the tumours and non-tumours using HOG algorithm?

RQ5. Can SVM classify the tumours and non-tumours correctly if the features from the images are extracted directly without the help of HOG?

1.3   THESIS ORGANIZATION

The outline of this thesis is briefly described in Chapter 1. Introduction along with our aim objective and research question is explained.

Chapter 2 explains the previous works that had been done on brain tumour detection.

Chapter 3 gives a deep understanding of Histogram of Oriented Gradients and Support Vector Machine.

Chapter 4, the implementation of the feature vector with SVM classifier is explained.

Chapter 5 shows the results of the analysis. In Chapter 6, thesis work is concluded by giving future scope on detection of a brain tumour.

CHAPTER 2.   RELATED WORK

Many works have been done on how to detect the brain tumours. In [2] authors had proposed a step by step approach for a brain tumour detection by differentiating healthy brain VS brain with tumours, benign VS malignant tumours and then followed by an algorithmic approach which consists of seven stages like image pre-processing, image segmentation, feature extraction and image classification using neural networks techniques. Their approach detected a tumour and defined the type of a tumour. Their techniques included canny edge detection and Harris, adaptive threshold and Harris. The technique canny edge detection and Harris showed 18.75% for falsely recognising healthy brain as well as a brain with a tumour and 10% for benign and malignant tumours. Second technique adaptive threshold and Harris showed 15.625% for falsely recognising healthy brain VS brain with a tumour and 6.25% for benign and malignant tumours

In [5] authors proposed textural feature extraction algorithm based on kurtosis (KWCEM) wavelet coefficient energy model for brain tumour extraction and detection. The algorithm was applied to high glioma (HG) and low glioma (LG) images. Their approach resulted in improvement of the quality of image segmentation and also reduced the feature set size. The algorithm was further used with canny edge detection which greatly increased the quality of the segmented image.

In [6] authors have proposed a comparative method for identifying brain tumours. Their approach included image mining techniques like (GLCM) Gray Level Co-Occurrence, Intensity-based Histogram features, Intensity-based features. The techniques were applied to BraTS database which showed good results in terms of accuracy. The techniques GLCM, Intensity-based Histogram features, Intensity-based features were compared with the J48 algorithm. GLCM showed 95.25 in accuracy whose value is very close to the J48 algorithm.

In [7] authors have proposed an algorithm as GUI that identifies a lesion, extracts and identifies it. The algorithm mainly uses Otsu method for creating a 3d image from a 2d image. The method showed detection of tumours and their shapes very accurately and effectively. Further, the method was compared with Multimodal MRI segmentation of ischemic. It showed good results in lesion assessment but needs refinement to achieve high sensitivity levels.

In [8] authors proposed a novel method for brain tumour detection and classification using Gabor wavelet and PNN. This method enabled feature extraction using wavelet transform. The classification of a tumour into malignant, metastatic and benign is achieved using PNN. Their approach resulted in a good accuracy of classifying the tumours.

In [9] authors proposed a four-step approach for a brain tumours classification. Their approach included pre-processing, Segmentation, feature extraction and classification. The classifications of tumours are done using a new technique TANN. This technique was applied to BraTS, OASTS and NBTR dataset. The classification time for BRATS dataset was comparatively less than other two. Their approach of TANN technique resulted in high detection rate and fast classification speed.

In [10] authors proposed a comparative method for a detection of a brain tumour. They compared segmentation techniques like mean shift, Thresholding by histogram through transform and SVM on both PET as well as MRI images. The results showed that for MRI images SVM and ThH are good in detecting the tumour whereas for PET SVM gave better results. The results were based on parameters like PSNR, Jaccard Index, dice Index and GCE.

In [11] authors proposed a hybrid approach for detection and classification of brain tumours. The hybrid approach involves four phases in which skull is detected in the first phase. In the second phase, they extracted the feature using grey level co-occurrence maintain. In the third phase, least square Support Vector Machine is used to classify the type of a tumour whereas in final phase segmentation was done. SVM results in an accuracy of 5.6% when compared with (RBF) Radial Basis Function and BP (WW).

In [12] authors proposed a neural network approach for detection of a brain tumour. Their approach involved noise reduction in MRI images, adaptive Thresholding techniques, segmentation the image using canny edge detection and classification using backpropagation as a base classifier. Their approach resulted in an accuracy of 90% in classifying the tumours compared to conventional method.

In [13] authors proposed a two-step approach for detection and classification of brain tumours an LCM is used for feature extraction whereas k-nearest neighbour classifier is used for classifying the tumours. Their results showed that K-NN has achieved highest accuracy of 96.15 when compared with other classifiers like backpropagation neural network, Radial basis, DWT and PCA ANN.

Segmentation of a brain tumour is based on tissue-specific for high-grade brain tumours. The principle idea of this paper is that segmentation is casted as classification task and for context information discriminative power is used. Classification forest (CF) is equipped with spatially non-local features to represent the data and for additional along with MRI channels, Classification Forest is provided with initial probability estimates for the single tissue classes. Initial probabilities are specifically based on patient and computed at test time based on a learned model of intensity. Context information for each data point is obtained by combining the initial probabilities and non-local features. This method is automatic having segmentation run time of 1-2 minutes range per patient. This paper used BraTS data set consisting of real and synthetic, High and low-grade tumour. For each of these data, sets evaluation is performed independently that is training and testing are done on that same dataset. Overall the results of this evaluation show that for a high-grade tumour it has higher segmentation quality and synthetic data has a better performance than real dataset [14, pp. 1-9].

In this paper, automatic segmentation of gliomas in 3D magnetic resonance images are presented using the fully automatic algorithm. In this method voxel, wise probabilistic classification of the volume is built using discriminative random decision forest framework. Multi-channel MR modules (T1, T2, T1C, FLAIR), spatial-prior and long-range comparisons with 3D regions are used in this method to discriminate lesions. The symmetric feature is introduced based on the factor that gliomas tend to develop

in an asymmetric way. Quantitative evaluation of data is done on BraTS segmentation challenge 2012 datasets and improved results over the state of art are demonstrated. In this paper, intensity normalisation is performed both on training and for prediction to calculate local image features. Intensity histogram of each sequence (T1, T2, T1C and FLAIR) is set as a reference case for each data group (BRATS_HG and BRATS_LG) later image features are calculated for each voxel. These features include local multi-channel intensities and long-range displaced box. Classification process in this paper is performed using discriminative random decision forest [14, pp. 10-13].

In this paper "Tumour-cut" method is used as segmentation method for brain tumour segmentation. This method is adapted to multimodal data to include edema segmentation. The user has to draw the maximum diameter of a tumour making tumour-cut method semi-automatic or semi-supervised. Drawing the maximum diameter takes about a minute of user-interaction time per case. Overall dice overlap with the expert segmentation for edema or infiltration is 0.36 +/-0.25 and overall dice overlap with the expert segmentation for tumour region is 0.69 +/- 0.20. In this method, it takes about 10-20 minutes of typical runtime for each case based on the size of a tumour [14, pp. 14-18].

Automatic segmentation of brain-tumour is proposed in this paper for reporting it to "BraTS 2012- multimodal Brain Tumour Segmentation Challenge" of MICCAI'12. Grey distribution of pixels (Gaussian mixture model, GMM) model is combined with edge information between two different classes of tissues in the brain. This method takes about 30 minutes of process time for one volume in MATLAB [14, pp. 19-23].

Two-stage techniques for segmentation of a brain tumour from multispectral human brain MRIs which is fully automatic is presented in this paper. A brain tumour, edema and other healthy brain tissues are modelled with training volumes by using their combined space characteristics. By a combination of Bayesian classification of the Gabor decomposition of the brain, MRI volume is used as the segmentation technique to produce an initial classification of brain tumours and the other classes. Initial classification is done using Markov Random Field (MRF) classification of the Bayesian output to resolve local homogeneities and impose smoothing constraint. This method shows good results of dice similarity coefficient of 0.56 for oedema and 0.668 for a brain tumour [14, pp. 24-27].

In this method, Hoo-Chang Shin tried to find a non-linear decision boundary to classify a tumour and edema using a joint approach of hybrid clustering and logistic regression. The sparse dictionary is used in this method to find the image intensity which is learned using spare auto-encoder. Different combinations of sparse dictionary show different characteristics of the tissue types [14, pp. 28-31].

This paper proposes Random Walker method with interaction for Magnetic Resonance brain tumour images segmentation. This method provides a tool which helps the user to conveniently modify the results iteratively apart from providing with final segmentation result. The typical RW algorithms shortcoming has been overcome in this method by extending RW to feature space for soft clustering, and then carry out pixel-wise segmentation in image space. This proposed method has been tested on T2-weighted, FLAIR sequence and contrast-enhanced T1-weighted multimodal brain MR-images [14, pp. 32-35].

Xavier Tomas-Fernandez and Simon K. Warfield from Children's Hospital Boston, Boston MA 02115, USA, states that '*Localizing and quantifying the volume of a brain tumour from magnetic resonance images is a key task for the analysis of brain cancer.*' With the source of using an existing model- Global Gaussian mixture for brain tissue segmentation, they had presented a contemporary algorithm for brain tissue segmentation and brain tumour detection. This tissue model they proposed combined the patient global intensity model with a population local intensity model derived from a reference to healthy subjects. They estimated the parameters which maximize the tissue maximum posterior probabilities by using Expectation-Maximization. With respect to our coupled global or local intensity model brain tumours were modelled as outliners. Brain tumours generally show abnormal intensity level compared to other healthy subjects in that same location, we assume tumours correspond with brain areas with low likelihood, making feasible brain tumour detection as outliners towards our coupled global or local intensity model. Brain tumour segmentation was validated using the 30 glioma patients scan from the training dataset from MICCAI BraTS 2012 challenge [14, pp. 36-40].

This paper proposes a fully automated method for channel-specific tumour segmentation in multi-dimensional images. The method that has been proposed in this paper represents a tumour appearance model for a multi-dimensional sequence that provides channel-specific segmentation of a tumour. The generative model proposed here shares information about the spatial location of the lesion among channels while making full use of the highly specific multi-modal signal of the healthy tissue classes for segmenting normal tissues in the brain. Apart from providing with the tissue types, this model includes the latent variable for each voxel encoding the probability of observing the tumour at that voxel. When specific spatial structures cannot be described sufficiently through population priors, this method extends the general "EM segmentation" algorithm in such situations. Simplified EM algorithm is concluded in this paper due to which estimating the tissue state and that also allows to enforce additional constraints for segmenting lesions that are either hyper or hypointense with respect to other tissues visible in the same image [14, pp. 41-48].

Generative-discriminative approach for multi-modal tumour segmentation that has been built in its generative part and on a generative statistical model for tumour appearance in multi-dimensional images has been evaluated using latent tumour class and its discriminative part has been evaluated using machine learning approach based on a random forest using long range features that are capable of learning the local appearance of brain lesions in multi-dimensional images. This approach combines advantageous properties from both types of learning algorithms. First, tumour related image features in a robust fashion that are invariant to relative intensity changes have been extracted by relying on a generative model encoding prior knowledge on expected physiology and path physiological changes. Second, image features extracted from the generative model representing tumour probabilities in the different image channels to an arbitrary image representation desired by the human interpreter through an efficient classification method that is capable of dealing with high-dimensional input data and that returns the desired class probabilities has been transformed [14, pp. 56-63].

This paper works on a generative approach for patient-specific segmentation of brain tumours across different MR modalities. Latent atlas approach method is the basis of this paper. The individual segmentation of each scan supports the segmentation of the ensemble by sharing common information. This common information, in the form of

a spatial probability map of the tumour location, is inferred concurrently with the evolution of the segmentation. The joint segmentation problem is solved via a statistically driven level-set framework. This method has been illustrated using an example application of multimodal and longitudinal brain tumour segmentation, reporting promising segmentation results [14, pp. 64-73].

CHAPTER 3.   THEORY

3.1   PHYSICS OF MRI

As we have learned from our introduction on Magnetic Resonance Images, MRI works on the property of magnetization of atomic nuclei. The external magnetic field which is uniform and powerful is applied on the tissue to be examined. This process is done to align the protons of water nuclei of the tissues; these protons are randomly oriented within the nuclei. This alignment is called magnetization [15]. Magnetization becomes unsettled due to the influence of external Radio Frequency (RF) energy. Through various relaxation processes, nuclei return to its resting alignment, by doing so RF energy is emitted. After a certain period of time, emitted signals are measured. The signal from each location in the imaged plane consists of frequency information which is converted to its corresponding intensity levels by the implementation of Fourier Transform. Later they are displayed in shades of grey arranged in a matrix form of pixels. The sequence of RF pulses applied and collected is varied and different types of images are created [15].

FIGURE 3.1.1 MRI SCAN [15]

3.1.1 DEFINITIONS RELATED TO MRI

REPETITION TIME (TR):

The time between transmitting an excitation pulse to the application of the next pulse i.e. time between the successive pulses [15].

TIME TO ECHO (TE):

The time between transmitting RF excitation pulse and the peak of the signal induced in the coil i.e. time between the delivery of the RF pulse and receipt of the echo signal [15].

LONGITUDINAL RELAXATION TIME:

The time constant to determine the rate at which excited protons return to equilibrium i.e. it is the time taken by the spinning protons to realign with external magnetic field [15].

TRANSVERSE RELAXATION TIME (T2):

The time constant to determine the rate at which, whether the excited protons reach equilibrium or will go out of phase with each other i.e. time taken for spinning protons to lose phase coherence in the field of nuclei which is spinning perpendicular to the main field [15].
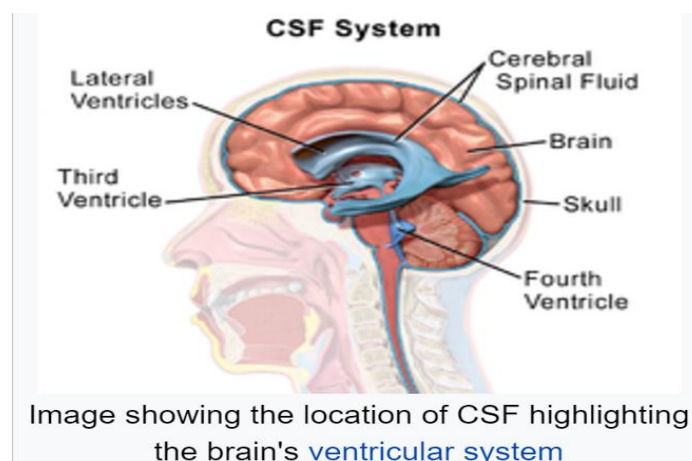
FIGURE 3.1.2 CSF SYSTEM

CEREBROSPINAL FLUID (CSF):

It is a colourless and clear body fluid present in the brain [15].

GADOLINIUM (GAD):

It is a non-toxic paramagnetic contrast enhancement agent. GAD when injected in to the body during a scan, it enhances and improves the quality of the MRI image. GAD enhanced images are especially useful in looking at vascular structures and breakdown in the blood-barriers [15].

3.1.2 MRI IMAGING SEQUENCE:

T1-WEIGHTED IMAGES:

T1- weighted images uses short TE and TR times. T1 properties of the tissues determine the contrast and the brightness of the image [15][16].
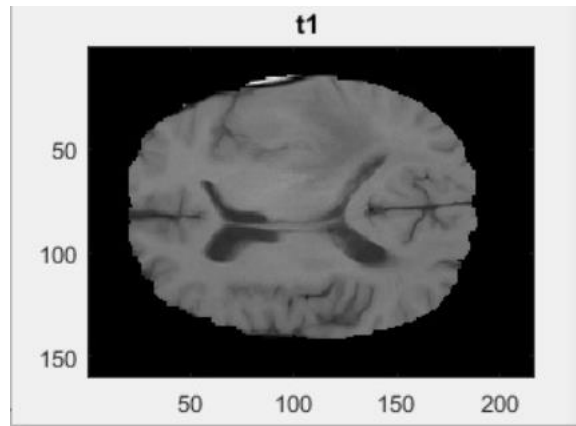
FIGURE 3.1.3 T1-WEIGHTED IMAGE

T2-WEIGHTED IMAGES:

T2-weighted images use longer TE and TR times. T2 properties of the tissues determine the contrast and the brightness of the image.
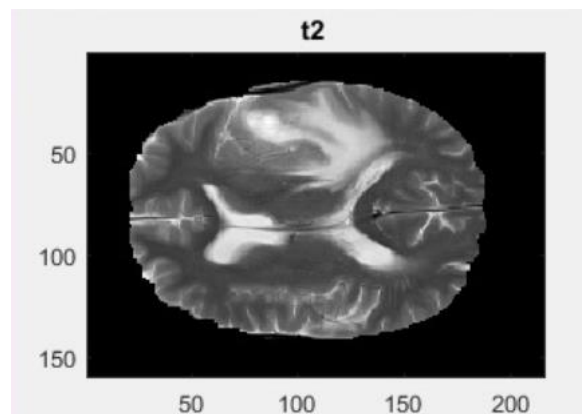
FIGURE 3.1.4 T2-WEIGHTED IMAGE

CSF is used to differentiate T1-weighted images and T2-weighted images, it is bright on T2-weighted images and dark on T1-weighted images [15][16].

FLUID ATTENUATED INVERSION RECOVERY (FLAIR):

FLAIR is similar to T2-weighted images but FLAIR has a very long TE and TR times due to which abnormalities remain bright but normal CSF fluid is attenuated and made dark. In this type of images abnormalities and CSF are differentiated because these

CSF and abnormalities are very sensitive to pathology. FLAIR has a better detection of the small hyperintense lesion [15][16].
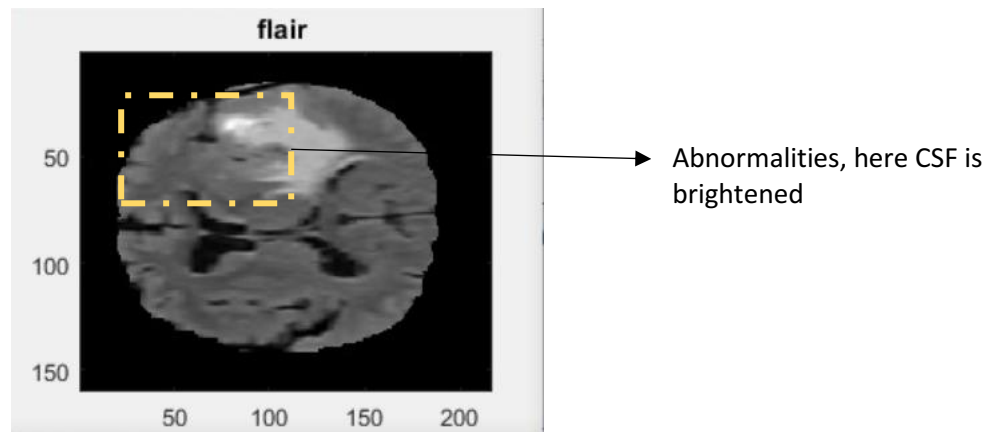
FIGURE 3.1.5 FLAIR IMAGE

MODALITIES	TR(msec)	TE(msec)
T1	500	14
T1-weighted images	4000	90
FLAIR	9000	114

TABLE I MODALITIES WITH TE AND TR VALES [15]

3.1.2.1 T1-WEIGHTED POST-GADOLINIUM CONTRAST (T1C) IMAGES:

T1-weighted images can also be performed while infusing Gadolinium. GAD is very bright on T1-weighted images.
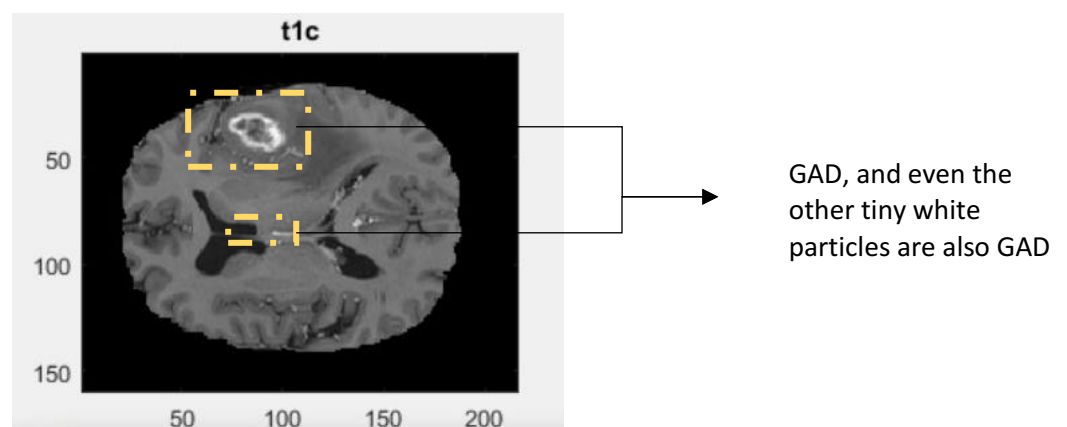
FIGURE 3.1.6 T1C-WEIGHTED IMAGE

Different RF pulse sequences can be used to highlight tissues in different ways. For example, a "T1-weighted" scan shows fluid as dark, and a "T2-weighted" scan shows fluid as bright. Fat will appear bright in both scans. Most pathological processes will

lower the fat content and raise the water content, so comparing the T1-weighted and T2-weighted scans (known as an irritation pattern) will highlight the matter [15].
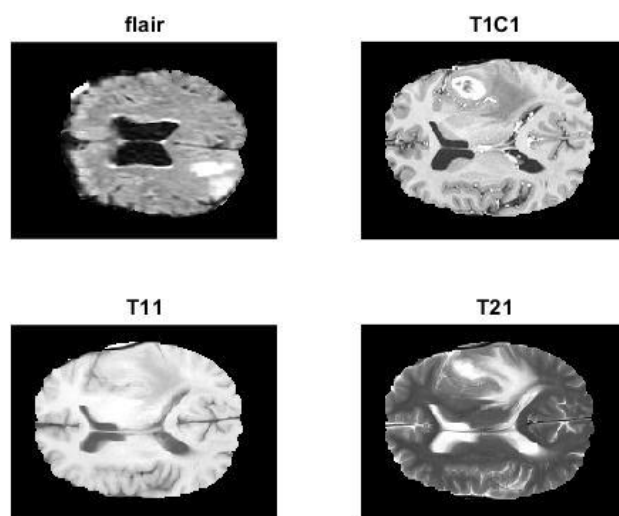
FIGURE 3.1.7 IMAGES SHOWING DIFFERENT MODALITIES OF SAME SLICE
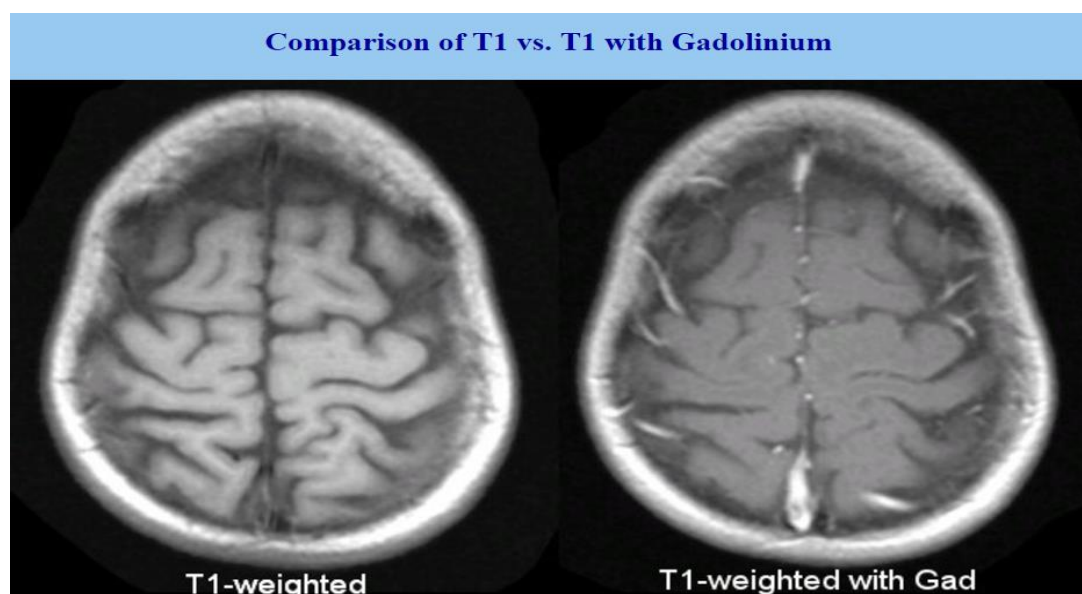
FIGURE 3.1.8 COMPARISON OF T1 VS T2

3.2   HISTOGRAM OF ORIENTED GRADIENTS (HOG)

Dalal and Triggs first introduced Histogram of Oriented Gradients to recognize a person in an image. HOG is a feature descriptor used in image processing for object detection purpose. The purpose of the feature descriptor is to generalise the object in an image such that this object produces the same feature descriptors in the images, containing that object, acquired under different conditions like different angle, illumination, distance etc.,. The HOG descriptor technique counts occurrences of

gradient orientation in localised portions of an image - detection window, or region of interest (ROI).

1. HOG initially divides the images into cells. Cells can be either rectangular or radial.
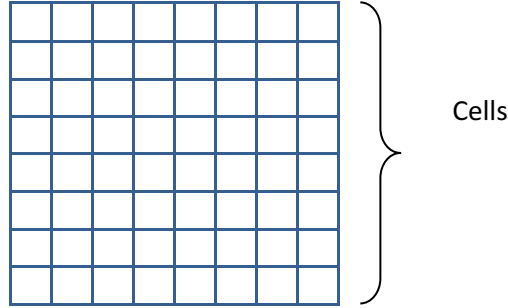
FIGURE 3.2.1 DIVISION OF IMAGE INTO CELL

2. For every pixel in the cell, gradient vector is calculated [17].

38	84	69	102	124	40
48	93	80	50	140	67
56		94	84	90	141
106	55	144	53	83	91
96	105	87	132	52	90
35	82	123	92	57	48

$\begin{bmatrix} 38 \\ 38 \end{bmatrix}$

These are the gradients in X and Y direction (see eq.3.1 and 3.2)
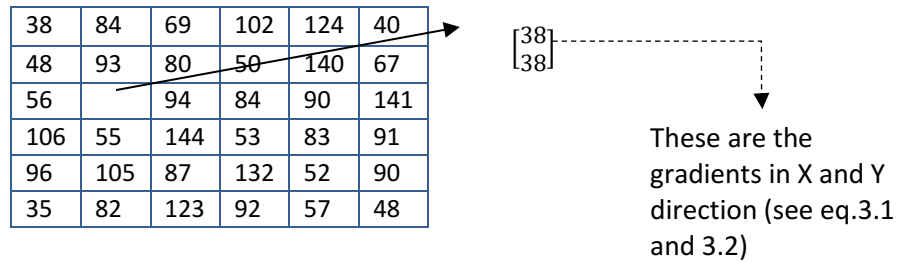
FIGURE 3.2.2 PIXEL VALUES IN ZOOMED VERSION OF A CELL

3.2.1 GRADIENT VECTOR:

The gradient vector is one of the important concepts in computer vision. The image gradient is another name for gradient vector [17].

3.2.1.1 APPLICATION OF GRADIENT VECTOR:

1. Edge detection
2. Feature extraction

Gradient vector at a particular pixel is calculated by taking the difference of neighbourhood values in both horizontal axis and vertical axis. Gradients can be subtracted from left to right or right to left in horizontal and top to bottom or bottom to top in vertical

$$\text{X-axis:} \quad 94\text{-}56\text{=}38 \tag{3.1}$$
$$\text{Y-axis:} \quad 93\text{-}55\text{=}38 \tag{3.2}$$

After calculating the gradient vectors for each and every pixel, magnitude is found out

$$\text{Magnitude} = \sqrt{X^2 + Y^2} \tag{3.3}$$
$$= \sqrt{38^2 + 38^2} \tag{3.4}$$
$$= 53.74 \tag{3.5}$$

Orientation plays a key role in HOG. Orientation can be termed as a change in direction, in which pixel intensity value changes. The change in direction can be along X-axis or Y-axis. The orientation of a gradient vector is calculated as

$$\text{Orientation} = arc \ tan\left(\frac{Y}{X}\right) \tag{3.6}$$

$$= arc \ tan\left(\frac{38}{38}\right) \tag{3.7}$$

$$= 0.785 \ radians \tag{3.8}$$

$$= 45 \ degrees \tag{3.9}$$

38	84	69	102	124	40
48	93	80	50	140	67
56		94	84	90	141
106	55	144	53	83	91
96	105	87	132	52	90
35	82	123	92	57	48

Orientates to 45 degrees
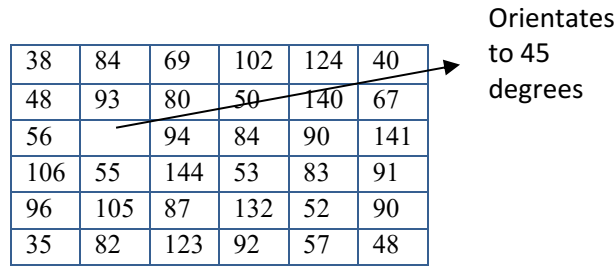
FIGURE 3.2.3 ORIENTATION OF PIXELS IN CELLS

The orientation of each and every pixel depends on the value of the gradient vector. The gradients are placed into bins of the histogram as per its orientation.

10	30	50	70	90	110	130	150	170

FIGURE 3.2.4 BINS IN HISTOGRAM

In the figure 3.2.3 the gradient vector has an angle of 45 degrees. We add 1/4th of its magnitude to the bin centred at 30 degrees, and 3/4ths of its magnitude to the bin centred at 50 as there are no 45 degrees bin the histogram [17].

3.2.2 NORMALISATION:
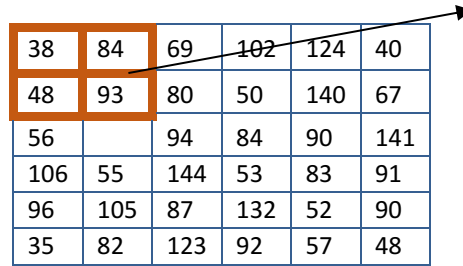
The magnitude of the gradient vector for pixels in an image varies. To have the same value, normalisation is done. Normalisation is defined as dividing the vector by its magnitude. Magnitude gets affected by normalisation whereas orientation is unaffected [17].

3.2.3 CELL REPRESENTATION:

The image is divided into cells of $m \times n$. The size of the cells can be taken as 2×2, 4×4, 6×6 and 8×8 pixels. The main reason for dividing the image into cells is compact representation [18].

3.2.4 BLOCK NORMALISATION:

Grouping of cells into the block is the basis for grouping and normalisation of histograms. Block histogram is the normalised group of cells. The main advantage of the calculating histogram on the blocks of an image is that it makes the image more robust to local variations in illumination.

38	84	69	~~102~~	124	40
48	93	80	50	140	67
56		94	84	90	141
106	55	144	53	83	91
96	105	87	132	52	90
35	82	123	92	57	48

FIGURE 3.2.5 BLOCK REPRESENTATION

3.2.5 FEATURE DESCRIPTOR:

The set of these block histograms represent the feature descriptor. Technically, a feature descriptor represents an image or a part of an image that simplifies the original form of an image by extracting the important information. The distribution of orientation of gradients is taken as features in HOG. Consider an image of size width × height × channels, feature descriptor coverts the size of the image into feature vector/length of the array [18].

3.3 SUPPORT VECTOR MACHINE OVER NEURAL NETWORK:

SVMs are equivalent to shallow neural network architecture but still, SVMs cannot add hidden layers to a network. SVM even requires more work on feature engineering compared to the neural network but the neural network is a very complex structure which requires more data for training compared to SVM because it has many layers. Since the data used in this thesis are less so SVM is preferable because it's less complex, the better solution at a faster date and cost is also less [26]

3.3.1 ADVANTAGES OF SVM:

- Accuracy
- High dimensionality as it works efficiently in high dimensional spaces ($\geq 10^6$).
- More efficient as it uses a subset training points.
- Works well on smaller and clean datasets.
- Memory efficient as only subsets of the training points are used in the decision process of assigning new members so only these points are stored in memory when making decisions [19] [20].

3.3.2 DISADVANTAGES OF SVM:

- Not suitable for larger datasets as the training time with SVM can be high.
- Performance of SVM is poor when a number of features for each object exceed the number of training data samples.
- Less effective on noisy datasets with overlapping classes.
- Non-probabilistic – since the classifier separates the objects by placing above and below the hyperplane there is no direct probabilistic interpretation for group

24

membership. However, one potential metric to determine "effectiveness" of the classification is how far from the decision boundary the new point is [19] [20].

3.3.3 USES OF SVM:

- Text classification tasks: category assignment, detecting spam and sentiment analysis.
- Image recognition challenges.
- Aspect-based recognition.
- Colour-based classification.
- Handwritten digit recognition (example: postal automation services)[19].

Support Vector Machine is a supervised machine learning algorithm used for data classification. SVM works on the idea of finding a hyperplane which divides the data set in the best possible way. This is explained using the figure 3.3.1 [19].
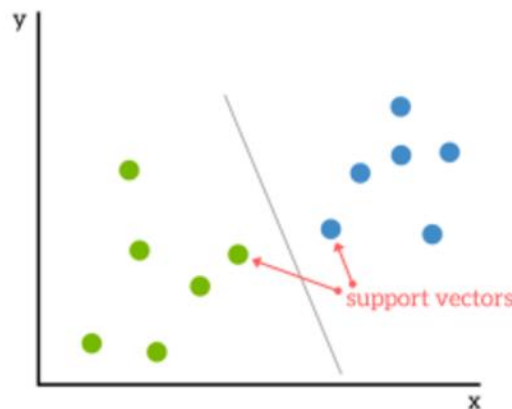
FIGURE 3.3.1 DATASET CLASSIFICATION BASED ON HYPERPLANE

SVM creates a finite dimensional feature space which is a vector space in which each dimension represents the 'feature' of a particular object. Collection of vectors is called a vector space [19].

3.3.4   SUPPORT VECTORS:
Support vectors are the data points that are nearest to the hyperplane. These points are crucial in deciding the position of a hyperplane that is dividing the data set [19].

3.3.5   HYPERPLANE:

The linear hyper plane is a geometrical entity which in a high dimensional feature space is an object one dimension lower than that space which divides the feature space into two regions [20]. Hyperplane is a plane that linearly separates a set of data. A simple classification with only two features is shown in Figure 3.3.2 [19].
New objects are above or below the hyperplane for categorisation based on features in the objects [19].
Linear separating hyperplane need not pass through the origin of our feature space that means zero vectors need not be included as an entity in the plane. This kind of hyperplanes are called affine. Formally, in mathematical language, SVM constructs linear separating hyperplanes in high dimensional vector spaces [20].
Data points are represented as $(\vec{x}, y)$

where
$$\vec{x} = (x_1 \ldots x_p) \qquad\qquad (3.10)\ [20]$$
x_j is the feature value

y= (+1 or -1) is the class of vector X classification

and we can consider that data points lie further from the hyperplane. The accuracy of the classification is judged on how well the separation happens. Since this is done intuitively we prefer data points to be as far as possible from the hyperplane, while still being on the correct side of it [20].

3.3.6 SEGREGATION OF CLASSES WITH THE DATA:

The margin is the distance between the hyperplane and nearest data point of either data set. Optimal classification occurs when the margin is large.
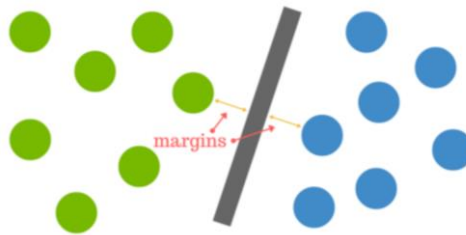
FIGURE 3.3.2 MARGIN

Data is not always as clear as the example shown above. Consider a condition where the sets overlap, data sets are not always linearly separable. We can classify the sets by converting a 2D image viewer into a 3D image viewer. Imagine the above-mentioned example where all the balls are lifted into the air and they are separated using a sheet. This launching of the balls into the air represents a mapping of data into higher dimensions. This process is called kernelling.
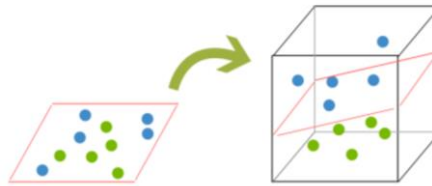
FIGURE 3.3.3 KERNELLING

Since the image is a 3dimesional image the hyperplane is a sheet and not a line. The idea is that the data will continue to be mapped into higher dimensions until a hyperplane can be formed to segregate it. For a *p*-dimensional feature space, represented as $\mathbb{R}^p$ then hyper plane is an affine p-1 dimensional space embedded within a *p*-dimensional feature space [19].

3.3.7 MAJOR GOALS OF SVM:

1. Train a model to assigns a new unseen object into a particular category.
2. A hyperplane with the greatest possible margin with any point of the training set and a greater chance of the new data being classified correctly.

We train the model by creating a linear partition of the feature space into two categories using hyperplane [19].

3.4   EVALUATION

3.4.1   LEAVE- ONE -OUT CROSS -VALIDATION:

In leave-one-out cross-validation; the available data is used for both training and testing. For example, if we have n samples of data, n-1 samples are used for training and left out sample is used for testing. The leave-one-out cross-validation is generally used to test the performance of recognition system when the data is limited [25].

3.4.2   RECEIVER OPERATING CHARACTERISTICS:

It is a plot of true positive rate against the false positive rate for different possible cut points (threshold) of a diagnostic test.
Receiver operating characteristics analysis was a part of Signal detection theory field which was developed during World War II for the analysis of radar images. Radar operator had to decide what category does the blip on the screen represents, whether it is a friendly ship or an enemy target or just a noise. Signal detection theory measures the ability of radar operator to make these important decisions. This ability was called receiver operating characteristics and hence it got its name ROC [21].

	Condition A	Condition NOT A
Test says A	True positive (TP)	False positive (FP)
Test says NOT A	False negative (FN)	True negative (TN)

TABLE II RECEIVER OPERATING CHARACTERISTICS [23]

TRUE POSITIVE RATE (TPR):

It is also known as sensitivity. It is defined as a measure of correctly identified in positive proportions (ratio of total positive points to total detected points) [22] [23].

$$TPR = \frac{TP}{(TP+FN)}$$ (3.11).

TRUE NEGATIVE RATE (TNR):

It is also known as specificity. It is defined as a measure of correctly identified in negative proportions [22] [23].

$$TNR = \frac{TN}{(FP+TN)}$$ (3.12).

FALSE POSITIVE RATE (FPR):

It is also known as expectancy. It is measured as a ratio between the number of negative events wrongly categorized as positive (false positive) and the total number of actual negative events (regardless of classification) [22] [23].

$$FP = 1 - specificity$$ (3.13).

$$\text{False positive rate: } \frac{FP}{N} = \frac{FP}{FP+TN} \tag{3.14}$$

FALSE NEGATIVE RATE (FNR):

This is a condition which actually happened but is claimed that it did not happen. That is wrongly concluding a negative about the condition [22].

$$\text{FNR= 1-TPR} \tag{3.15}$$

$$Accuracy = \frac{TN+TP}{(TP+FP+TN+FN)} \tag{3.16}$$

CHAPTER 4.   IMPLEMENTATION

Database selection for brain tumour images

↓

Feature extraction of brain tumour images using HOG

↓

Labelling of the features extracted from the HOG

↓

Feeding of the labelled features to the SVM

↓

Classification of brain images into tumour (1) or no-tumour (0) using SVM

↓

Performance test of SVM based on ROC characteristics

↓

Accuracy, sensitivity and specificity values for each modality based on ROC curve

FLOW CHART 1 OUR APPROACH TO BRAIN TUMOR DETECTION.

The flow chart 1 shows the approach to brain tumour detection. Initially, database which contains brain images has to be selected. The second step is to extract the features from brain images using HOG. Next step is to label the extracted features and feeding to SVM. Then, SVM classifies the tumour and non tumour. Final step is to test the performance of SVM based on ROC characteristics accuracy, sensitivity and specificity.

4.1   EVALUATION DATABASE:

We implemented the algorithms on the non-licensed database i.e., BraTS. BraTS database was accessed through the registration student information. The database shows that brain has an unpredictable shape and appearance which is usually challenging for using these brain images in medical image analysis [24]. Comparison of existing tumour segmentation method is hard because the input datasets vary a lot based on features like structural MR contrasts, perfusion or diffusion data etc.

In order to overcome this problem Acropolis Convention Centre- Nice, France has organized a Multimodal Brain Tumour Segmentation (BraTS) challenge in conjunction with the MICCAI2012 conference [14]. A large dataset of brain tumour MR scans which consist of a tumour and edema regions which are manually delineated had been made available for this purpose. They also provided computer-generated brain tumour images generally called as synthetic images. These synthetic images also have corresponding ground truth images.

In this database, all the brain images are of high glioma or low glioma type. They consist of three different folders they are: challenging data, individual observer or ground truth and training data.

FLOW CHART 2 CONTENTS OF BRATS DATABASE

The flow chart 2 shows the division of database into three subfolders Individual observer, Challenging data and Training data which contain the brain images.

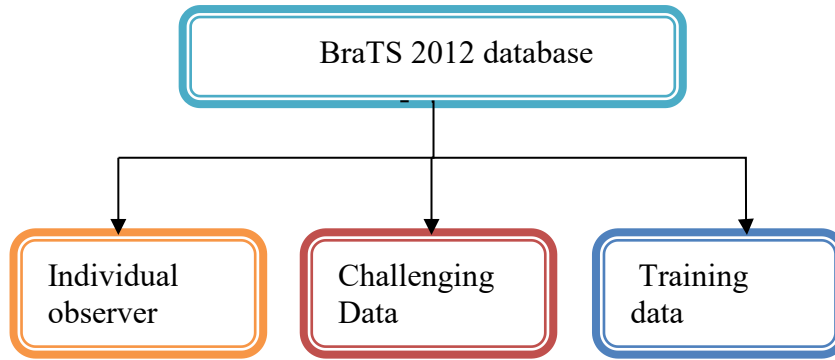Individual observers which are the ground truth images consist of 4 observers named observer1, observer2, observer3, and observer4. These sub-folders (i.e., observer1, observer2, observer3, and observer4) of the observer folder provide with the information regarding 20 high glioma and 10 low glioma brain tumour images so a total count of 30 glioma images in each observer resulting in 30*4=120 glioma images (see flow chart 3). They are the ground truth images which give information regarding four modalities FLAIR, T1, T1C and T2 respectively. All these ground truth images are sorted as signed 16-bit integers [24].
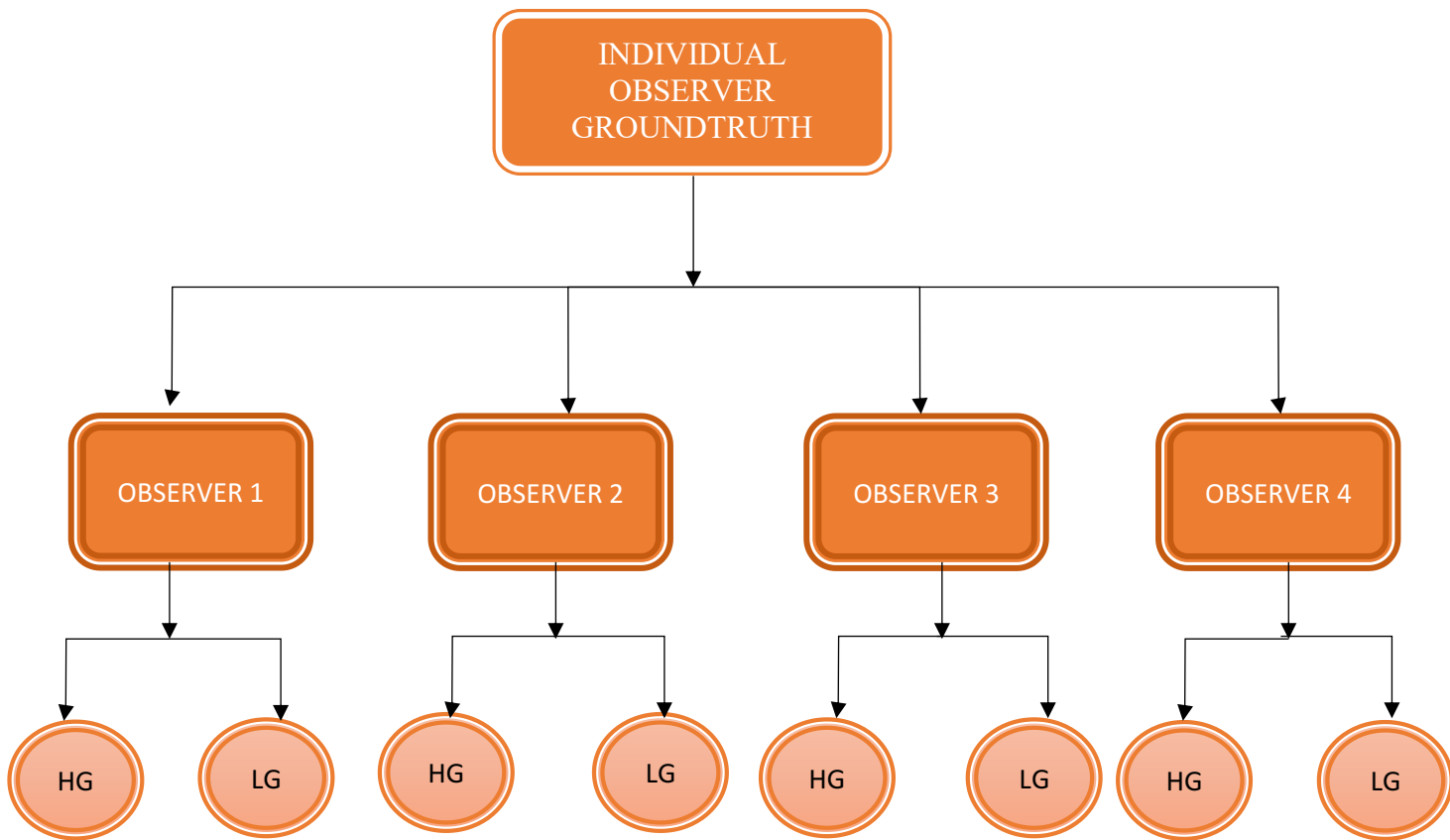
FLOW CHART 3 CONTENTS OF INDIVIDUAL OBSERVER GROUND TRUTH DATA

Flow chart 3 shows the four subfolders observer 1, observer 2, observer 3 and observer 4 of Individual Observer Ground Truth folder. Each observer subfolder has high glioma brain images and low glioma brain images

Ground truth images of image data folder are manually segmented using the indexes 0, 1,2,3,4 having the labels as follows (as shown in figure 4.1):
Index 1 representing necrosis,
Index 2 representing edema,
Index 3 representing non-enhancing tumour,
Index 4 representing enhancing tumour,
Index 0 representing everything else,
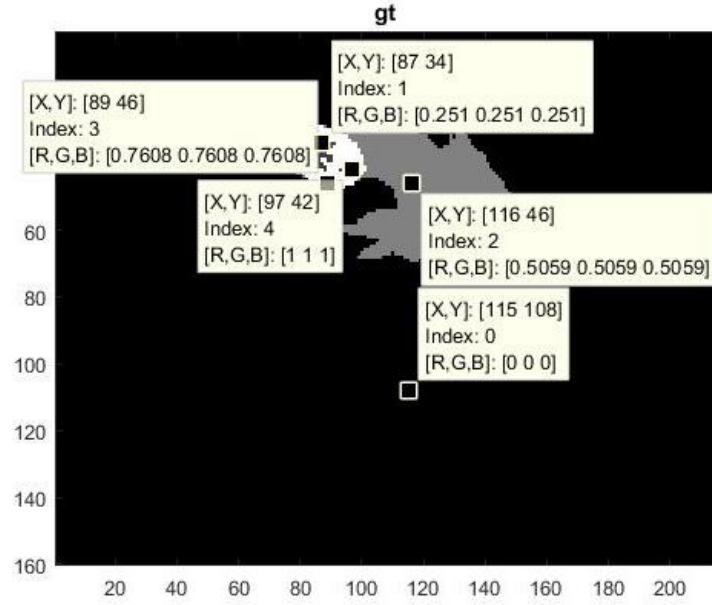
FIGURE 4. 1 IMAGE WITH ALL INDEXES

Ground truth images of synthetic data folder are manually segmented using the indexes
0, 1and 2 having the labels as follows:
Index 1 represents edema,
Index 2 represents tumour core and
Index 0 represents everything else.
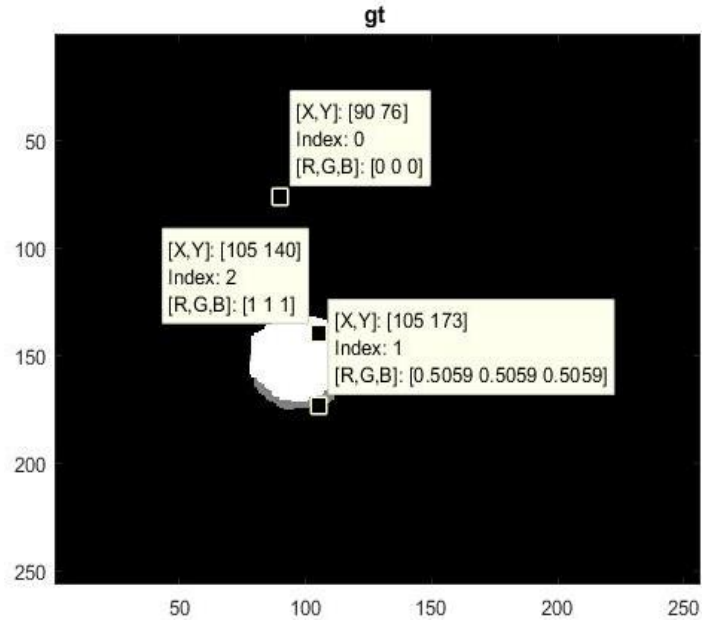
FIGURE 4.2 IMAGE WITH 0, 1, 2 INDEXES
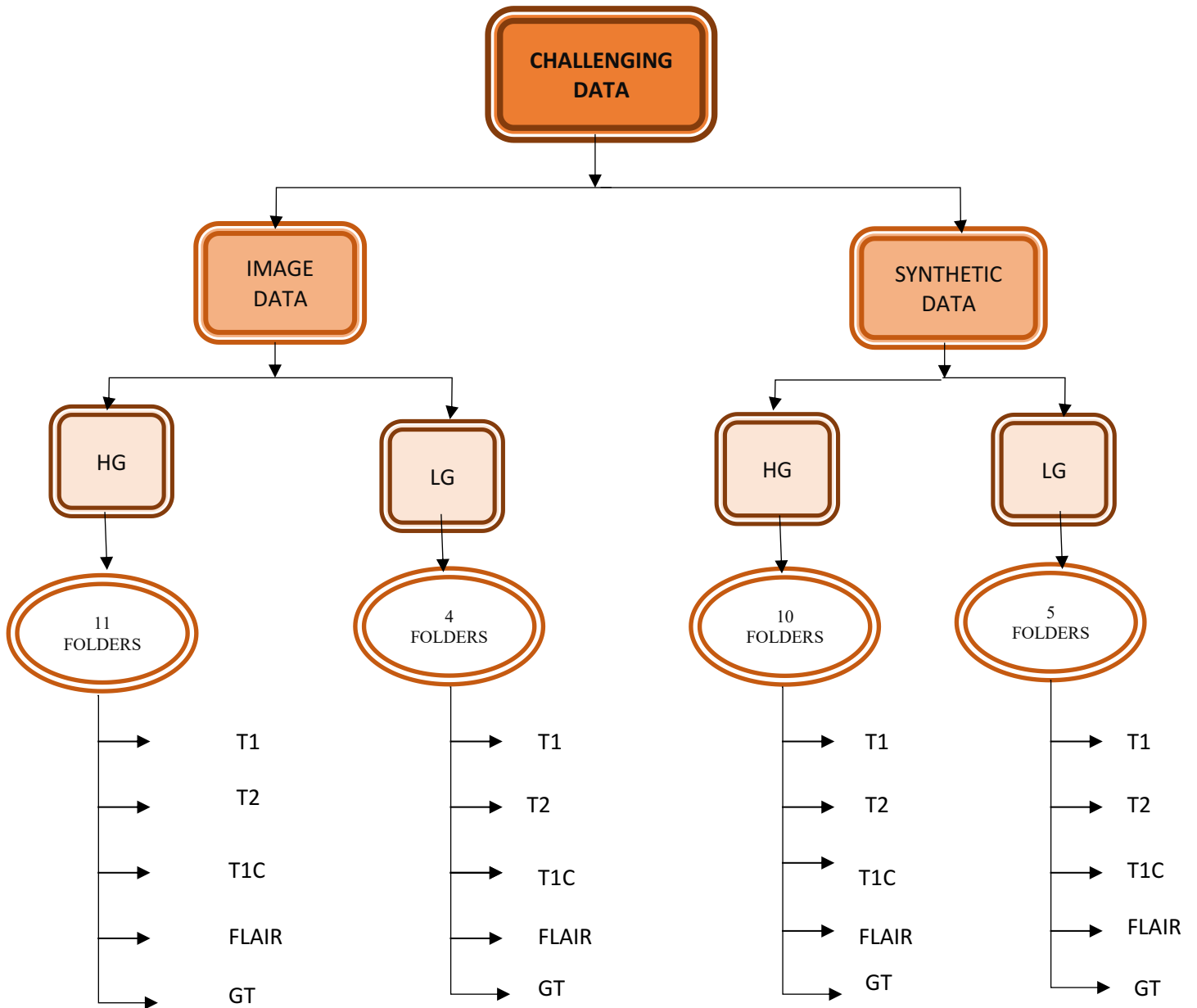
FLOW CHART 4: CHALLENGING DATA FOLDER

Flow chart 5 shows BraTS2 challenge folder consists of image data and synthetic data where image data has high glioma and low glioma subfolders and the same with synthetic data also.

High Glioma folder of image data has 11 folders which consist of 4 .mha folders each belonging to FLAIR, T1, T1C and T2.

Low Glioma folder of image data has 4 folders which consist of 4 .mha folders each belonging to FLAIR, T1, T1C and T2.

High Glioma folder of synthetic data has 10 folders which consist of 4 .mha folders each belonging to FLAIR, T1, T1C and T2.

Low Glioma folder of synthetic data has 5 folders which consist of 4 .mha folders each belonging to FLAIR, T1, T1C and T2 [24].
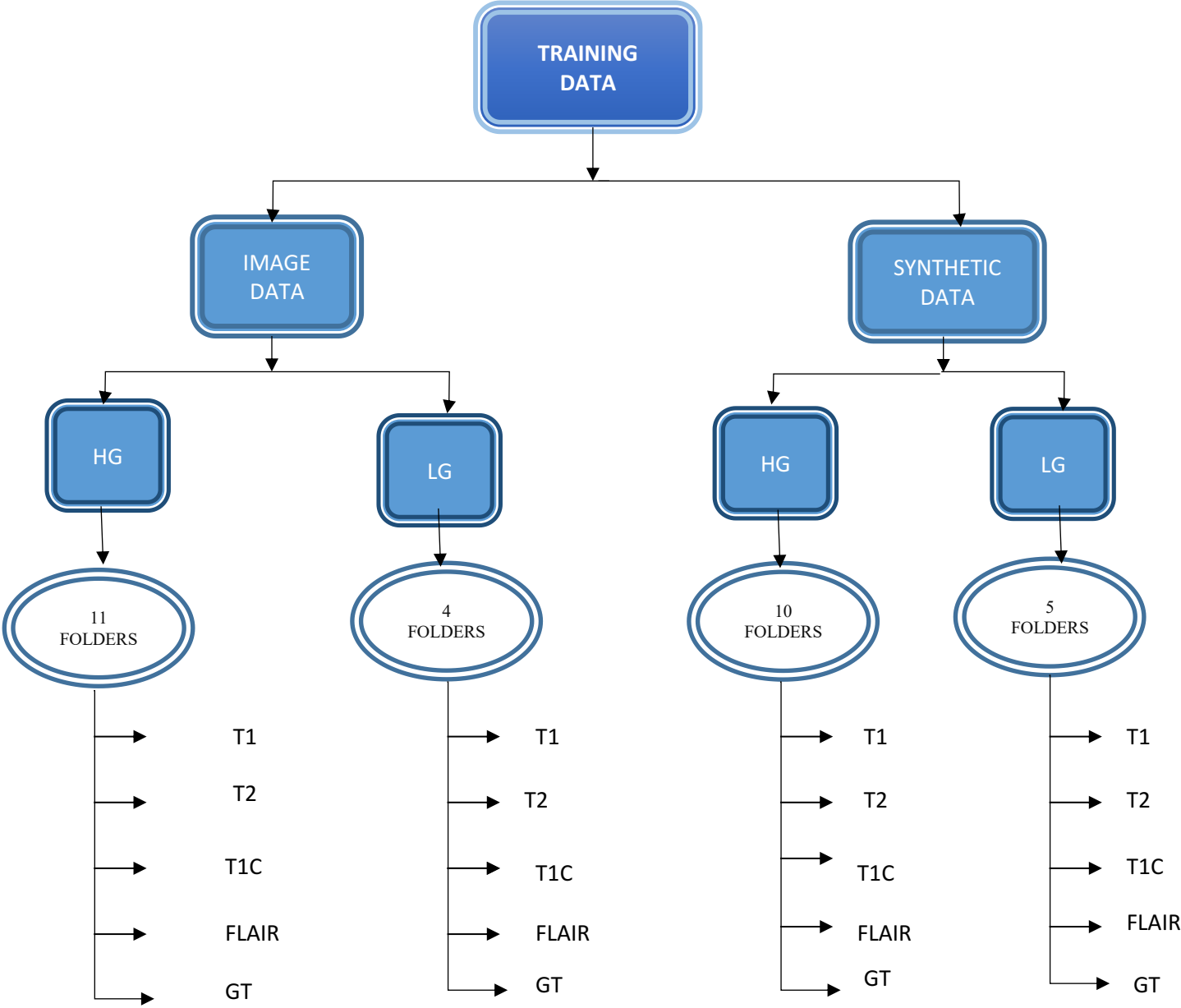
FLOW CHART 5 TRAINING DATA FOLDER

The flow chart 5 shows BraTS2 training folder consists of image data and synthetic data where image data has high glioma and low glioma subfolders and the same with synthetic data also.

High Glioma folder of image data has 20 subfolders which consist of 5 .mha folders each belonging to FLAIR, T1, T1C, T2 and Ground Truth.

Low Glioma folder of image data has 10 subfolders which consist of 5 .mha folders each belonging to FLAIR, T1, T1C, T2 and Ground Truth.

High Glioma folder of synthetic data has 20 subfolders which consist of 5 .mha folders each belonging to FLAIR, T1, T1C, T2 and Ground Truth.
Low Glioma folder of synthetic data has 10 subfolders which consist of 5 .mha folders each belonging to FLAIR, T1, T1C, T2 and Ground Truth [24].

All the images in the database are of .mha format. We cannot import .mha format files directly in MATLAB, therefore the MATLAB functions mha_read_reader and mha_read_volume are used.
Each image consists of an average of 176 slices. Some of the slices have the presence of a tumour (as seen in figure 4.4) where some slices are empty (as seen in figure 4.3).

FIGURE 4.3 SLICE OF BRAIN TUMOUR IMAGE WITH NO INFORMATION
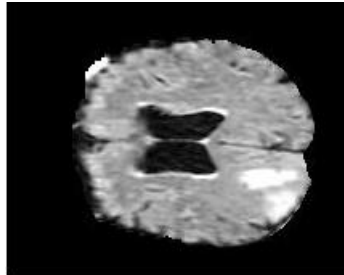
FIGURE 4.4 SLICE OF BRAIN TUMOUR IMAGE, A SECTION OF BRAIN

We considered 40th to 130th slice of every image with a difference of 5 slices between them instead of each and every slice because these slices has information of the indexes 1, 2, 3 and 4. The index 4 (enhancing tumour) of ground truth image in image data folder is considered as the basis to know whether a tumour is present or not in modalities like FLAIR, T1, T1C and T2 whereas index 2 of ground truth images in synthetic image folder is considered as basis to know whether a tumour is present or not in modalities like FLAIR, T1, T1C and T2. Only index 4 is considered as vital among other indexes because the cancer form, represented by pixels with index 4 is the most dangerous and difficult to treat when compared to others [24].

4.2   FEATURE EXTRACTION USING HOG:

1. A cell size of [4 4] is taken as an optimum one because if we increase the cell size to [8 8] we might lose small-scale information.

2. Each slice of every image in the database is represented by one feature vector, consisting of 74412 values.

3. Features within the range 4500 to 65000 have values whereas before and after that range have zero values which can be eliminated.

4. Some of the .mha files have dimensions 160×216×176, 176×216×176, 168×240×240, 162×230×230.

5. To avoid mismatch while extracting features from images, we resized all the images to 160×216.

4.3   FEATURE EXTRACTION USING A SLICE IN THE IMAGE:

1. In the method, feature extraction using a slice in the image, the features are extracted directly from the slices of an image without the help of HOG. The feature from each slice of an image is extracted as follows,

x_1y_1	x_1y_2	x_1y_3	x_1y_4	x_1y_5	....	x_1y_n
x_2y_1	.....	....	....	.....	....	....
x_3y_1	......	....	....	......	....	......
x_4y_1	......	.....	....	....	....	....
x_5y_1	....	.....	....	....	....	....
x_6y_1	....	....	....	....	....	....
:						
x_ny_1	....	......	....	....	....	x_ny_n

FIGURE 4.5 MATRIX OF SLICE OF AN IMAGE

Here, x=number of rows
y=number of columns

2. As shown in figure 4.5, matrix of pixels of slice of an image dimension (x_n, y_n) is converted to column vector in figure 4.6, with each column containing ($x_ny_n \times 1$) features.

3. For better understanding, there are ten images in LG subfolder of image data folder. As explained in 4.1, each image has an accurate of 176 slices, the features from the same slice number (ex: 60) of all ten images are extracted and stored as ($10 \times x_ny_n$).

4. The extracted ($10 \times x_ny_n$) features are fed as input to SVM.

5. In the same way the features of different slices of the images are extracted and fed to SVM.

$$
\begin{array}{|c|}
\hline
x_1 y_1 \\
\hline
x_2 y_1 \\
\hline
x_3 y_1 \\
\hline
x_4 y_1 \\
\hline
x_5 y_1 \\
\hline
x_6 y_1 \\
\hline
\vdots \\
\vdots \\
\vdots \\
\vdots \\
\vdots \\
\hline
x_n y_1 \\
\hline
\end{array}
$$

FIGURE 4.6 FEATURE VECTOR (which is a column of pixels in one slice)

4.4 CLASSIFICATION OF THE FEATURE VECTORS BY SVM:

1. To detect an object in an image the features of the image have to be fed to a recognition system which in this work is SVM.

2. We stored the features of slices of every image of HG and LG sub folders of training data folder to feed them to SVM.

3. We created a .mat file which has the labels for the images indicating 'a tumour' or 'no tumour'

4.5 PERFORMANCE OF SVM:

1. The performance of SVM is tested based on ROC characteristics as described in Section 3.4.2.

2. The original values which are obtained based on examining ground truth images are stored in 'labels' as '1' for 'tumour' and '0' for 'no tumour' and outputs from SVM are stored into 'scores' which are also in binary format.

3. Only the HG and LG images of Training data folder are considered for training and testing the SVM.

CHAPTER 5. RESULTS AND ANALYSIS

As explained in chapter 3 leave one cross one validation was used for testing the performance of Support Vector Machine on images of the modalities FLAIR, T1C, T1 and T2 of training folder in the database. The ROC characteristics true positive rate, true negative rate, false positive rate and false negative rate were calculated. From ROC characteristics accuracy, sensitivity and specificity values were calculated and are shown in tables III-VIII.

5.1   IMAGE DATA HG-INDEX4

TABLE III IMAGE DATA HG-INDEX4

IMAGE DATA HG-INDEX 4												
	ACCURACY (%)				SENSITIVITY				SPECIFICITY			
Slice. NO	FLAIR	T1C	T1	T2	FLAIR	T1C	T1	T2	FLAIR	T1C	T1	T2
40	47.37	36	36	36	0	0	0	0	0.947	0.736	0.736	0.735
45	38.9	36.11	38.9	38.9	0	0	0	0	0.778	0.722	0.778	0.78
50	44.45	38	36.11	36.11	0	0	0	0	0.889	0.778	0.722	0.722
55	44.12	32.35	52	29.41	0	0	0.3	0	0.882	0.647	0.71	0.588
60	44.12	38	65	29.41	0	0	0.6	0	0.882	0.76	0.647	0.588
65	46.43	59.3	59.3	59.3	0	0.33	0.3	0.25	0.928	0.857	0.857	0.937
70	47.62	39.28	47.62	47.62	0.166	0	0.167	0.166	0.785	0.785	0.785	0.785
75	45.24	41.76	48.9	55.2	0.142	0.142	0.28	0.14	0.762	0.692	0.69	0.961
80	45.05	37.91	59.8	52.74	0.285	0.142	0.42	0.285	0.615	0.615	0.76	0.76
85	65	50	55	50	0.8	0.5	0.7	0.6	0.5	0.5	0.4	0.4
90	56	59.89	52	63.7	0.692	0.769	0.76	0.84	0.428	0.428	0.28	0.42
95	50	50	50	50	1	1	1	1	0	0	0	0
100	50	50	50	50	1	1	1	1	0	0	0	0
105	50	50	50	50	1	1	1	1	0	0	0	0
110	65	50	53	50	0.933	0.6	0.6	1	0.4	0.4	0.4	0
115	46.87	43.75	46	43	0.937	0.875	0.93	0.86	0	0	0	0
120	54	62	63	42.8	0.928	0.928	0.928	0.857	0.17	0.33	0.34	0
125	54	46.43	46	42.8	0.928	0.928	0.928	0.857	0.17	0	0	0
130	63.74	63	54.3	74.7	0.428	0.428	0.85	0.57	0.846	0.847	0.23	0.92
135	56	56	**87**	74.7	0.8	0.8	0.8	0.57	0.33	0.33	0.94	0.92

The table III shows the accuracy, sensitivity and specificity values of the modalities FLAIR, T1C, T1 and T2 of high glioma images for slices in each image ranging from 40 to 135 with an interval of 5 slices. If we observe the values, SVM gave an accuracy of 87% for a 135th slice of T1 modality with the high sensitivity of 0.8 and specificity of 0.94 whereas FLAIR, T1c modalities showed 56% with a sensitivity of 0.8 and specificity of 0.33. For the same 135th slice, SVM gave 74.7% in accuracy for T2 modality with a sensitivity of 0.57 and specificity of 0.92. SVM classified the images of T1 modality into tumours and non-tumours with high accuracy where it failed to classify the images of FLAIR and T1c modalities at least to a close accuracy of T1 modality.

5.2 IMAGE DATA LG-INDEX 4

TABLE IV IMAGE DATA LG-INDEX 4

IMAGE DATA LG-INDEX 4											
	ACCURACY (%)				SENSITIVITY				SPECIFICITY		
Slice. NO	FLAIR	T1C	T1	T2	FLAIR	T1C	T1	T2	FLAIR	T1C	T1	T2
90	62	43.75	43.75	43.75	0.5	0	0	0	0.75	0.87	0.87	0.87
100	50	52.2	52	52	0	0.3	0.3	0.3	1	0.7	0.7	0.7
110	37.5	43.75	50	50	0	0	0	0	0.75	0.87	1	1
120	43.75	43.75	50	50	0	0	0	0	0.87	0.87	1	1
130	50	50	50	50	0	0	0	0	1	1	1	1

The table IV shows the accuracy, sensitivity and specificity values of the modalities FLAIR, T1C, T1 and T2 of low glioma image data folder ranging from 90 to 130 with a gap of 10 slices. Observe the values of image data log, SVM gave an accuracy of 62% for a 90th slice of FLAIR modality with a sensitivity of 0.5 and specificity of 0.75 whereas T1c, T1 and T2 modalities showed 43.75% with a sensitivity of 0 and specificity of 0.87. SVM could not classify the tumours into tumours correctly for T1c, T1 and T2 modalities. So, the sensitivity is 0 for T1c, T1 and T2 modalities. SVM is able to classify the tumours into tumours correctly for FLAIR modality with a sensitivity of 0.5. If we consider 100,110 120 and 130th slices of FLAIR modality SVM again fails to classify the tumours to tumours exactly and showed a sensitivity of 0 because the slices within range 100 to130 have index 0,1 ,2 and 3 which are not useful as index 4. 100th slice of T1c modality stood next after 90th slice of FLAIR modality in achieving an accuracy of 52.2% with sensitivity of 0.3 and specificity of 0.7

5.3 SYNTHETIC DATA HG-INDEX 2

TABLE V SYNTHETIC DATA HG-INDEX 2

SYNTHETIC DATA HG-INDEX 2											
	ACCURACY (%)				SENSITIVITY				SPECIFICITY		
Slice. NO	FLAIR	T1C	T1	T2	FLAIR	T1C	T1	T2	FLAIR	T1C	T1	T2
100	66.15	60.13	66.15	66.15	0.823	0.8235	0.823	0.823	0.5	0.375	0.5	0.5

The table V shows the accuracy, sensitivity and specificity values of a 100th slice of every image of the modalities FLAIR, T1C, T1 and T2 from high glioma synthetic data folder. The reason for only calculating accuracy, sensitivity and specificity values of a 100th slice of every image of synthetic data folder without choosing other slices is they do not have information regarding index 2. As we have explained in the section 4.1 that only index 0, index 1 and index 2 are there for synthetic folder images in which cancer form of index 2 pixels are more dangerous. For the synthetic data folder of HG, SVM classified the tumours into tumours correctly for FLAIR, T1 and T2 modalities with a sensitivity of 0.823 by showing an accuracy of 66.15%. For T1c modality, SVM showed an accuracy of 60.13% with a sensitivity of 0.823 and a specificity of 0.375 which is not bad when compared to other modalities.

5.4 SYNTHETIC DATA LG-INDEX 2

TABLE VI SYNTHETIC DATA LG-INDEX 2

SYNTHETIC DATA LG-INDEX 2											
	ACCURACY (%)				SENSITIVITY				SPECIFICITY			
Slice. NO	FLAIR	T1C	T1	T2	FLAIR	T1C	T1	T2	FLAIR	T1C	T1	T2
100	45.5	53.34	53.34	67	0.578	0.738	0. 738	0.684	0.33	0.33	0.33	0.67

Table VI shows the accuracy, sensitivity and specificity values of a 100th slice of every image of the modalities FLAIR, T1C, T1 and T2 from low glioma synthetic data folder. If we consider T2 modality of synthetic data folder SVM gave an accuracy of 67% by classifying tumours to tumours with a sensitivity of 0.7. SVM failed to classify tumours to tumours for FLAIR modality and showed an accuracy of 45% with a sensitivity of 0.5.

5.5 IMAGE DATA HG IN VECTOR FORM INDEX 4

TABLE VII IMAGE DATA HG IN VECTOR FORM INDEX 4

IMAGE DATA HG-INDEX 4												
	ACCURACY (%)				SENSITIVITY				SPECIFICITY			
Slice. NO	FLAIR	T1C	T1	T2	FLAIR	T1C	T1	T2	FLAIR	T1C	T1	T2
90	66	48.35	45.05	66.48	0.4	0.538	0.615	0.615	0.933	0.428	0.285	0.714
95	94.5	86.84	**97.37**	50	0.89	0.736	0.947	1	1	1	1	1
100	38.5	38.89	38.87	44.44	0.77	0.777	0.777	0.888	0	0	0	0
105	36	41.66	41.66	44.44	0.72	0.833	0.833	0.888	0	0	0	0
110	23	30	40	46.66	0.46	0.6	0.4	0.733	0	0	0.4	0.2
115	37.5	31.25	31.25	43.75	0.75	0.625	0.625	0.875	0	0	0	0
120	59.5	52.38	44.05	52.38	0.857	0.714	0.714	0.214	0.33	0.333	0.166	0.833
125	49	48.81	48.81	45.23	0.642	0.642	0.642	0.571	0.34	0.333	0.333	0.333
130	52.5	45.05	52.74	56.59	0.287	0.285	0.285	0.285	0.77	0.615	0.769	0.846
135	66.7	86.66	90	66.66	0.4	0.8	0.8	0.4	0.93	0.933	1	0.933

As explained in subchapter 4.3, different feature vectors are used as compared to 5.1-5.4. The table VII shows the accuracy, sensitivity and specificity values of the modalities FLAIR, T1C, T1 and T2 of high glioma image data folder ranging from 90 to 135 with a gap of 5 slices between them. If we observe the values of image data HG in vector form, SVM gave an accuracy of 97% for a 95th slice of T1 modality with a sensitivity of 0.9474 and specificity of 1 among all modalities.

5.6   IMAGE DATA LG IN VECTOR FORM INDEX 4

TABLE VIII IMAGE DATA LG IN VECTOR FORM INDEX 4

IMAGE DATA LG-INDEX 4												
	ACCURACY (%)				SENSITIVITY				SPECIFICITY			
Slice. NO	FLAIR	T1C	T1	T2	FLAIR	T1C	T1	T2	FLAIR	T1C	T1	T2
90	50	56.2	20.83	68.75	0.5	0.5	0	0.5	0.5	0.62	0.625	0.875
100	28.6	42.8	28.57	42.85	0	0	0	0	0.572	0.85	0.571	0.857
110	43.75	43.7	43.75	43.75	0	0	0	0	0.875	0.87	0.875	0.875
120	37.5	37.5	37.5	31.25	0	0	0	0	0.75	0.75	0.75	0.625
130	50	44.4	44.44	50	0	0	0	0	1	0.88	0.888	1

As explained in subchapter 4.3,different feature vectors are used as compared to 5.1-5.4. The table VIII shows the accuracy, sensitivity and specificity values of the modalities FLAIR, T1C, T1 and T2 of low glioma image data folder ranging from 90 to 130 with a gap of 10 slices between them. If we observe the values of image data LG in vector form, SVM gave an accuracy of 68.75% for a 90th slice of T2 modality with a sensitivity of 0.5 and specificity of 0.875 among all modalities. The image data folder of LG could not give a good accuracy for the modalities when compared to the image data folder of HG.

CHAPTER 6. CONCLUSIONS

The main part of the thesis was on how to extract features from brain tumour images using a histogram of oriented gradients followed by a classification method, Support Vector Machine.

Middle slices of high glioma images of image data folder have the complete information about index 4 but SVM failed to give a high accuracy in this condition. 135th slice of T1 modality was classified by SVM with a highest accuracy of 87% only. SVM in this condition cannot acquire 100% accuracy.

Support Vector Machine failed to identify tumour images correctly for low glioma images of image data folder and had shown a sensitivity value 0 for most of the modalities. SVM could not classify the synthetic data folder images correctly due to the presence of index 0 in most of the images, as index 0 has no information. For low glioma images SVM could only acquire an average accuracy of 50% with a specificity of 0.33.

Whereas, the features extracted from HG images directly without the help of histogram of oriented gradients gave a highest accuracy of 97%, sensitivity 0.94 and specificity 1 for high glioma images. Accuracy, sensitivity and specificity of low glioma images are 68.75%, 0.5 and 0.875 respectively. Support Vector Machine had shown a better classification in this condition by acquiring greater values compared to those values obtained using features extracted from images using HOG.

The computational time is greater for synthetic folder compared to image data folder as the synthetic folder has more number of images to extract the features. Finally, we conclude that brain tumours can be detected with the help of histogram of oriented gradients by a classifier, Support Vector Machine. The method is more suitable for detecting brain tumours in high glioma images than low glioma images.

CHAPTER 7. FUTURE WORK

Research on brain tumour detection can also be extended in other ways:

➢ The ROC characteristics accuracy, sensitivity and specificity of SVM in classifying tumours and non-tumours can be improved further for low glioma images.
➢ To extract the features of images instead of the histogram of oriented gradients, one can use local binary pattern and log Gabor algorithms.
➢ To test the performance of SVM on other databases for an improvement in accuracy, sensitivity and specifcity values.
➢ Classifiers like k- nearest neighbour, Bayes quadratic, Bayes linear and neural network can also be used in classifying the tumours and non-tumours.

REFERENCES

[1] "Brain Tumors (Benign and Malignant): Symptoms, Causes, Treatment," *WebMD*. [Online]. Available: https://www.webmd.com/cancer/brain-cancer/brain-tumors-in-adults.

[2] E. F. Badran, E. G. Mahmoud, and N. Hamdy, "An algorithm for detecting brain tumors in MRI images," in *The 2010 International Conference on Computer Engineering Systems*, 2010, pp. 368–373.

[3] "Brain Tumor: Symptoms, Signs, Treatment, Surgery & Types." [Online]. Available: https://www.medicinenet.com/brain_tumor/article.htm.

[4] "Brain Tumor: Diagnosis," *Cancer.Net*, 25-Jun-2012. [Online]. Available: https://www.cancer.net/cancer-types/brain-tumor/diagnosis.

[5] D. S. Parameshwari and P. Aparna, "An efficient algorithm for textural feature extraction and detection of tumors for a class of brain MR imaging applications," in *2014 19th International Conference on Digital Signal Processing*, 2014, pp. 339–344.

[6] B. S. Kumar and R. A. Selvi, "Feature extraction using image mining techniques to identify brain tumors," in *2015 International Conference on Innovations in Information, Embedded and Communication Systems (ICIIECS)*, 2015, pp. 1–6.

[7] R. Noureddine, K. Tarhini, and S. Saleh, "Segmentation and extraction of brain injury lesions from MRI images: Matlab implementation," in *2015 International Conference on Advances in Biomedical Engineering (ICABME)*, 2015, pp. 45–48.

[8] "Two dimensional discrete Wavelet transform and Probabilistic neural network used for brain tumor detection and classification - IEEE Conference Publication." [Online]. Available: http://ieeexplore.ieee.org/document/7893235/.

[9] "Real Brain Tumors Datasets Classification using TANNN - 2cb07be69a673ff55bb5ddd39c637b7c31d6.pdf.".

[10] M. G. Sumithra and B. Deepa, "Performance analysis of various segmentation techniques for detection of brain abnormality," in *2016 IEEE Region 10 Conference (TENCON)*, 2016, pp. 2056–2061.

[11] "Hybrid approach for brain tumor detection and classification in magnetic resonance images - IEEE Conference Publication." [Online]. Available: http://ieeexplore.ieee.org/document/7437900/.

[12] K. Kaur, G. Kaur, and J. Kaur, "Detection of brain tumor using NNE approach," in *2016 IEEE International Conference on Recent Trends in Electronics, Information Communication Technology (RTEICT)*, 2016, pp. 1864–1868.

[13] N. V. Chavan, B. D. Jadhav, and P. M. Patil, "Detection and Classification of Brain Tumors," *Int. J. Comput. Appl.*, vol. 112, no. 8, pp. 48–53, Feb. 2015.

[14] B. Menze, A. Jakab, S. Bauer, M. Reyes, M. Prastawa, and K. V. Leemput, *Proceedings of the MICCAI Challenge on Multimodal Brain Tumor Image Segmentation (BRATS) 2012*. MICCAI, 2012.

[15] "MRI Basics." [Online]. Available: http://casemed.case.edu/clerkships/neurology/Web%20Neurorad/MRI%20Basics.htm.

[16] "What is the difference between MRI scans T1, T1c, T2, FLAIR ?..." [Online]. Available: https://www.researchgate.net/post/What_is_the_difference_between_MRI_scans_T1_T1c_T2_FLAIR_Is_there_another_type_of_scan.

[17] "HOG Person Detector Tutorial · Chris McCormick." [Online]. Available: http://mccormickml.com/2013/05/09/hog-person-detector-tutorial/.

[18] "Histogram of Oriented Gradients | Learn OpenCV." [Online]. Available: https://www.learnopencv.com/histogram-of-oriented-gradients/.

[19] "Support Vector Machines: A Simple Explanation." [Online]. Available: https://www.kdnuggets.com/2016/07/support-vector-machines-simple-explanation.html.

[20] "Support Vector Machines: A Guide for Beginners | QuantStart." [Online]. Available: https://www.quantstart.com/articles/Support-Vector-Machines-A-Guide-for-Beginners.

[21] "Plotting and Intrepretating an ROC Curve." [Online]. Available: http://gim.unmc.edu/dxtests/roc2.htm. [Accessed: 23-Oct-2017].

[22] "Receiver operating characteristic - Wikipedia." [Online]. Available: https://en.wikipedia.org/wiki/Receiver_operating_characteristic.

[23] "roc - Relation between true positive, false positive, false negative and true negative - Cross Validated." [Online]. Available: https://stats.stackexchange.com/questions/61829/relation-between-true-positive-false-positive-false-negative-and-true-negative.

[24] "BRATS - SICAS Medical Image Repository." [Online]. Available: https://www.smir.ch/BRATS/Start2015.

[25] "How does leave-one-out cross-validation work? How to select the final model out of n different models? - Cross Validated." [Online]. Available: https://stats.stackexchange.com/questions/27454/how-does-leave-one-out-cross-validation-work-how-to-select-the-final-model-out.

[26] "Machine Learning: What are advantages of SVM over Neural networks and k-Nearest neighbours?" [Online]. Available: https://www.quora.com/Machine-Learning-What-are-advantages-of-SVM-over-Neural-networks-and-k-Nearest-neighbours.